

## Evaluation of Main Parameters in Re-Entry Trajectories \*

S. Sgubini<sup>a</sup>, G.B. Palmerini<sup>a</sup>

<sup>a</sup> “Sapienza” - Università di Roma  
Scuola di Ingegneria Aerospaziale

### Abstract

---

The selection of the descending path for re-entry vehicles presents serious challenges for the designer. Basic requirements in terms of flight mechanics, dealing with initial and terminal conditions, have to match strict requirements related to the survivability of the re-entering body, in terms of structural integrity as well as in terms of thermal input and accepted temperature raise. The possibility of aero-braking assistance, allowed only if the targeted celestial body is surrounded by an atmosphere, increases the degrees of freedom available to the designer. The paper focuses on this special case, looking for an evaluation of the critical parameters (maximum load factor, maximum thermal flux) with respect to the flight dynamics of the trajectory.

The initial step is represented by a procedure proposed by Broglio to approximately identify the initial conditions for suitable descent trajectories as function of a limited number of parameters. The solutions do not depend explicitly on the shape of the body, and the approximations involved are quite reasonable, as shown by a comparison with purely numerical integration. The present papers builds on this approach by modifying the analytical process to better handle the flight phases close to the deceleration peak, which are the most critical ones. Some examples are included to show the advantages of the proposed approach.

---

### 1. Introduction

Reentry has been an important research area since the beginning of the manned space exploration. Then, the quest for more economical and efficient space transportation systems, leading to the re-usable launcher concept and specifically to the Shuttle, has provided the support for the re-entry related studies. More recently, the extended activity onboard of the International Space Station, with an increasing number of experiments involving biological material exposure to space environment conditions (radiations, zero-gravity) and the desire to analyse in large, equipped labs on the Earth their findings were the main drivers to keep alive the topic. Also to remember some - limited in number, but with great significance - special missions recovering deep space related material (Genesis, Hayabusa) that included a re-entry phase. It is clear that, with the advances in space techniques, the mastering of re-entry discipline will be mandatory to have an effective flow of people and products (medicines or high tech materials synthesized in gravity-less conditions) from orbit down to Earth. An additional reason to study is represented by the increased risk of poorly (or not-at-all) controlled spent or exhausted spacecraft (space debris) which of course

could be better managed by an in-depth knowledge of re-entry physics. The main issue in studying re-entry has been always related to the determination of safe condition with respect to the high thermal and structural loads generated along the descent. Fundamentals results have been obtained by Allen and Eggers for nonlifting bodies [1], while for lifting bodies Chapman proposed [2] to describe the descent by means of an auxiliary function ( $Z$  in literature) depending on the lift to drag ratio and on the entry conditions, to be - in general - evaluated numerically. Overall, the problem can be tackled by long software runs simulating the complete dynamics of the descent from specific initial conditions, each of them unfortunately adding a quite limited amount of information to the complete understanding of the problem. Instead, as already proposed by the authors [3], an approach based on the basic quantities (thermal and structural) of interest would greatly benefit the design phase. This path is followed in the present paper by taking into account the fundamental contribution by Broglio who, by means of the introduction of non-dimensional variables, described the descent in a general manner, based on structural and thermal peak values and not depending on the specific characteristics of the re-entering body ([4], [5]). The present paper improves, by means of a series expansion, the accuracy of the solutions already proposed, especially in the neighbourhood of the peak,

---

\*Based on paper presented at the XXII Congresso Nazionale AIDAA, Settembre 2013 Napoli, Italia

<sup>1</sup>©AIDAA, Associazione Italiana di Aeronautica e Astronautica

i.e. of the most challenging phase.

The following material includes (section 2) a short reminder of the kinematics and dynamics relations relevant to the descent trajectory, and necessarily reports part of the work by Broglio. Then the series expansion, which is this paper's specific contribution, is introduced. Several examples, referred to different conditions to show the performance of the approach, complete the description (section 3).

## 2. Analysis of the Descent

### 2.1. Kinematics

The choice of a reference frame - body centered - as the one depicted in figure 1 leads to the positions

$$\mathbf{r} = r\hat{\mathbf{r}} \quad \mathbf{V} = \dot{r}\hat{\mathbf{r}} + r\dot{\theta}\hat{\boldsymbol{\theta}} \quad (1)$$

offering for the acceleration

$$\mathbf{a} = (\ddot{r} - r\dot{\theta}^2)\hat{\mathbf{r}} + (2\dot{r}\dot{\theta} + r\ddot{\theta})\hat{\boldsymbol{\theta}} \quad (2)$$

By using

$$\dot{r} = -V \sin \theta \quad r\dot{\theta} = V \cos \theta \quad (3)$$

the two components of the acceleration read as

$$a_n = -(\ddot{r} - r\dot{\theta}^2) \cos \theta - (2\dot{r}\dot{\theta} + r\ddot{\theta}) \sin \theta \quad (4)$$

$$a_o = (2\dot{r}\dot{\theta} + r\ddot{\theta}) \quad (5)$$

or, in a form suitable for computation,

$$\begin{aligned} a_n &= - \left[ V \sin \theta \frac{d(V \sin \theta)}{dr} - \frac{V^2 \cos^2 \theta}{r} \right] \cos \theta - \\ &- \left[ -2 \frac{V^2 \sin \theta \cos \theta}{r} - rV \sin \theta \frac{d}{dr} \left( \frac{V \cos \theta}{r} \right) \right] \sin \theta = \\ &= -V \sin \theta \cos \theta \frac{d(V \sin \theta)}{dr} + \\ &+ \frac{V^2 \cos \theta}{r} (\cos^2 \theta + 2 \sin^2 \theta - \sin^2 \theta) + \\ &+ V \sin^2 \theta \frac{d}{dr} (V \cos \theta) = \\ &= \frac{V^2 \cos \theta}{r} + V \sin \theta (-\sin \theta \cos \theta \frac{dV}{dr} - \\ &- V^2 \cos^2 \theta \frac{d\theta}{dr} + \sin \theta \cos \theta \frac{dV}{dr} - V^2 \sin^2 \theta \frac{d\theta}{dr}) V = \\ &= \frac{V^2 \cos \theta}{r} - V^2 \theta \frac{d\theta}{dr} = V^2 \cos \theta \frac{dV}{dr} [\log(r \cos \theta)] = \\ &- \frac{V^2 \cos \theta}{2} \frac{d}{dr} [\log \frac{1}{r^2 \cos^2 \theta}] = - \frac{V^2 r^2 \cos^3 \theta}{2} \frac{d}{dr} [\frac{1}{r^2 \cos^2 \theta}] \end{aligned} \quad (6)$$

$$\begin{aligned} a_o &= -2 \frac{V^2 \sin \theta \cos \theta}{r} - rV \sin \theta \frac{d}{dr} \left( \frac{V \cos \theta}{r} \right) = \\ &= -2 \frac{V^2 \sin \theta \cos \theta}{r} + \frac{V^2 \sin \theta \cos \theta}{r} - \\ &- V \sin \theta \frac{d}{dr} (V \cos \theta) = \\ &= -V^2 \sin \theta \cos \theta \left[ \frac{1}{r} + \frac{1}{V \cos \theta} \frac{d}{dr} (V \cos \theta) \right] = \\ &= -V^2 \sin \theta \cos \theta [\log(rV \cos \theta)] \end{aligned} \quad (7)$$

### 2.2. Dynamics

The two non-trivial projections of the equation of motion read as

$$ma_n = -L + g \cos \theta \quad ma_o = -D \cos \theta + L \sin \theta \quad (8)$$

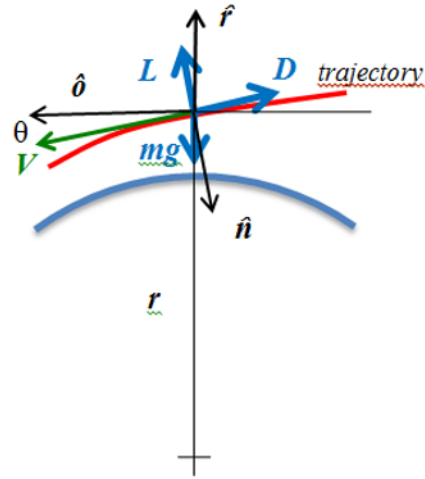


Figure 1. Frames of reference

Assuming the classical definitions for lift and drag

$$D = \frac{1}{2} C_D A \rho V^2 \quad L = \frac{1}{2} C_L A \rho V^2 \quad (9)$$

it is possible to write, by substituting the kinematic relations (6) and (7),

$$- \frac{V^2 r^2 \cos^3 \theta}{2} \frac{d}{dr} \left[ \frac{1}{r^2 \cos^2 \theta} \right] = - \frac{L}{m} + g \cos \theta \quad (10)$$

$$-V^2 \cos \theta \cos \theta \frac{d}{dr} [\log(rV \cos \theta)] = - \frac{D}{m} \cos \theta + \frac{L}{m} \sin \theta \quad (11)$$

Introducing the ballistic coefficient and the angular momentum

$$K = \frac{C_D A}{m} \quad w = rV \cos \theta \quad (12)$$

the two equations become

$$r^2 \frac{d}{dr} \left[ \frac{1}{r^2 \cos^2 \theta} \right] = - \frac{K \rho}{\cos^3 \theta} \frac{L}{D} - \frac{2gr^2}{w^2} \quad (13)$$

$$\frac{d \log w^2}{dr} = \frac{K \rho}{\sin \theta} \left( 1 - \frac{L}{D} \tan \theta \right) \quad (14)$$

The parameters of greatest interest for the design of the descending probe are the structural load factor and the thermal input. As far as it concerns the load factor

$$n = \frac{\sqrt{L^2 + D^2}}{mg_{\oplus}} = \frac{K \rho V^2}{2 g_{\oplus}} \sqrt{1 + \frac{L^2}{D^2}} \quad (15)$$

that attains the maximum value at (vanishing the time derivative)

$$\frac{2}{V} \frac{dV}{dt} + \frac{1}{\rho} \frac{d\rho}{dt} - V \sin \theta \frac{d \log \sqrt{1 + \frac{L^2}{D^2}}}{dr} = 0 \quad (16)$$

Substituting into (16) the relations

$$\frac{dV}{dt} = g \sin \theta - \frac{K}{2} \rho V^2 \quad \frac{d\rho}{dt} = \beta \rho V \sin \theta \quad (17)$$

being  $\beta = 1/H$ , with  $H$  the scale height of the selected exponential atmospheric model, the condition to attain the maximum (indicated with  $*$ ) becomes

$$2g \sin \theta - K \rho V^2 + \beta \rho V^2 \sin \theta - V^2 \sin \theta \frac{d \log \sqrt{1 + \frac{L^2}{D^2}}}{dr} = 0 \quad (18)$$

and then

$$\left( \frac{K \rho}{\sin \theta} \right)_* = \left( \beta + \frac{2g}{V^2} - \frac{d \log \sqrt{1 + \frac{L^2}{D^2}}}{dr} \right)_* \quad (19)$$

Evaluating the velocity from Eq.(15)

$$\frac{V^2}{g_\oplus} = \frac{n}{K \rho \sqrt{1 + \frac{L^2}{D^2}}} \quad (20)$$

the Eq.(19) can be expressed as

$$\left( \frac{K \rho}{\sin \theta} \right)_* = \frac{\beta - \left( \frac{d \log \sqrt{1 + \frac{L^2}{D^2}}}{dr} \right)_*}{1 - \frac{\sin \theta_*}{n_*} \frac{g_*}{g_\oplus} \left( \frac{d \log \sqrt{1 + \frac{L^2}{D^2}}}{dr} \right)_*} \approx \beta \quad (21)$$

where the approximation holds whenever  $L/D$  does not change suddenly.

Introducing the set of non-dimensional variables:

$$\xi = 1 - \frac{r_*}{r} \quad U = \frac{w_*^2}{w^2} \quad X = \frac{\sin \theta_*}{\sin \theta} \quad Y = \frac{\cos \theta_*}{\cos \theta} \quad (22)$$

$$\frac{L}{D} = \frac{\lambda}{\tan \theta_*} f(\xi) \quad \alpha = \beta r_*$$

and exploiting the approximation (21) the dynamics (Eqs. (13)-(14)) can be rewritten as

$$\frac{d}{d\xi} \left[ (1 - \xi)^2 Y^2 \right] + \frac{\alpha \sin \theta_*}{\bar{n}_*} U - \alpha \lambda f(\xi) Y^3 e^{-\alpha \frac{\xi}{1-\xi}} = 0 \quad (23)$$

$$\frac{d \log U}{d\xi} + \frac{\alpha e^{-\alpha \frac{\xi}{1-\xi}}}{(1 - \xi)^2} [X - \lambda f(\xi) Y] = 0 \quad (24)$$

with initial conditions  $U = X = Y = 1$  at  $\xi=0$  (i.e. at the load peak), allowing for a forward and backward integration from a defined, engineering-significant condition. The load factor can be reported to the local value of the gravitational attraction,

$$\bar{n}_* = \frac{n_*}{\frac{r_\oplus^2}{r_*^2} \left( \sqrt{1 + \frac{L^2}{D^2}} \right)_*} \quad (25)$$

Interestingly, Eqs (23) and (24) do not depend on the shape of the descending body ( $K$  does not appear anymore).

### 2.3. Thermal Problem

Indicating the radius of curvature of the re-entering capsule as  $R_{body}$ , the heat flux is

$$q = \frac{q_o}{\sqrt{R_{body}}} \left( \frac{\rho}{\rho_\oplus} \right)^{1/2} \left[ \frac{g_\oplus}{R_\oplus} \right]^3 = \frac{q_u}{\sin \theta_*} \left[ \frac{Y(1-\xi)g_\oplus}{\sqrt{U}} \sqrt{n_*} \right]^3 e^{-\frac{\alpha}{2} \frac{\xi}{1-\xi}} \quad (26)$$

where  $q_o=108836000$  if  $q$  is in  $W/m^2$ , and

$$q_u = \frac{q_o}{\sqrt{R_{body}}} \left( \frac{\alpha}{K r_* \rho_\oplus} \right)^{1/2} \left[ \frac{2}{\alpha} \right]^{3/2} \quad (27)$$

The total amount of heat transferred to the body is

$$Q = Q_u \left[ \frac{1}{\sin \theta_*} \right]^{3/2} n_* \int_{1 - \frac{r_*}{R_\oplus}}^1 \frac{XY^2}{U} e^{-\frac{\alpha}{2} \frac{\xi}{1-\xi}} d\xi \quad (28)$$

where

$$Q_u = q_u \sqrt{\frac{\alpha}{2}} \sqrt{\frac{r_*}{g_\oplus}} \quad (29)$$

### 2.4. Series Expansion

Previous relations basically recall the theory proposed by Broglio ([4], [5]). This approach can be improved by expanding as series the functions  $U$  and  $Y$  (both depending on variable  $\xi$  in order to better fit the behavior close to the altitude where the peak load is attained ( $\xi=0$ ):

$$Y = 1 + \frac{dY}{d\xi} \Big|_* \xi + \frac{1}{2} \frac{d^2 Y}{d\xi^2} \Big|_* \xi^2 + \frac{1}{6} \frac{d^3 Y}{d\xi^3} \Big|_* \xi^3 + \frac{1}{24} \frac{d^4 Y}{d\xi^4} \Big|_* \xi^4 + \dots \quad (30)$$

$$U = 1 + \frac{dU}{d\xi} \Big|_* \xi + \frac{1}{2} \frac{d^2 U}{d\xi^2} \Big|_* \xi^2 + \frac{1}{6} \frac{d^3 U}{d\xi^3} \Big|_* \xi^3 + \frac{1}{24} \frac{d^4 U}{d\xi^4} \Big|_* \xi^4 + \dots \quad (31)$$

The values of the derivatives of  $Y$  and  $U$  with respect to  $\xi$  are known, based on the dynamics, following

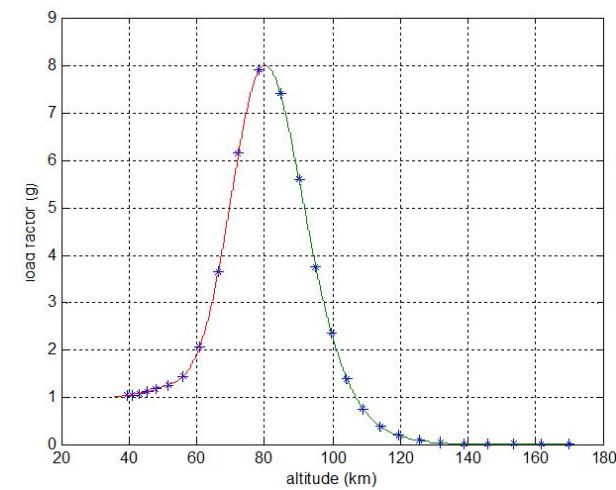
$$\frac{dY}{d\xi} = F(\xi, Y, U) \quad \frac{dU}{d\xi} = G(\xi, Y, U) \quad (32)$$

and the chain rule for derivation can be applied to further derivatives (similarly for  $U$ )

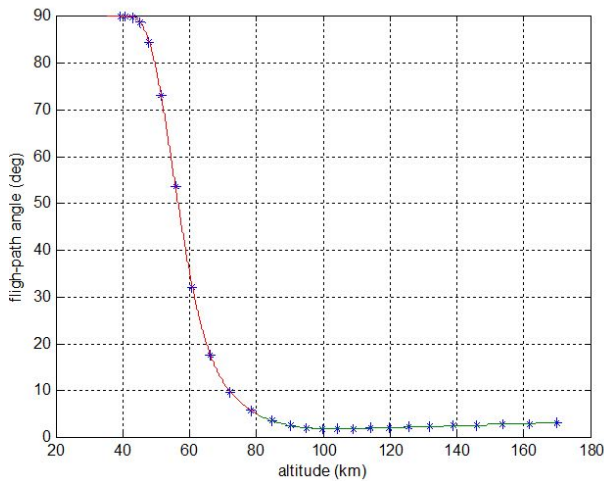
$$\frac{d^2 Y}{d\xi^2} = \frac{\partial F}{\partial \xi} + \frac{\partial F}{\partial Y} \frac{\partial Y}{\partial \xi} + \frac{\partial F}{\partial U} \frac{dU}{d\xi} \quad (33)$$

To be noticed that all these derivations can be easily carried on by means of symbolic computing. To be also remarked that, once  $Y$  has been selected for the series expansion and evaluated up to a given order, the companion variable  $X$  can be computed using the relation

$$\frac{\sin^2 \theta_*}{X^2} + \frac{\cos^2 \theta_*}{Y^2} = 1 \quad (34)$$



(a) Load factor



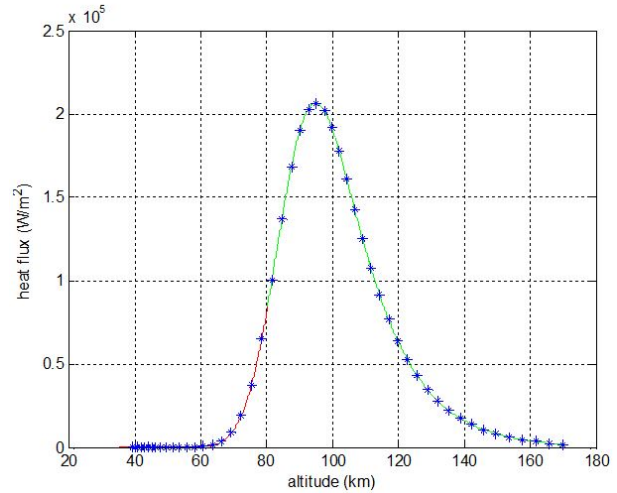
(b) Flight path angle

Figure 2. Parameters evaluated with the proposed approach and compared to data points from the numerical integration of the equations of motion.

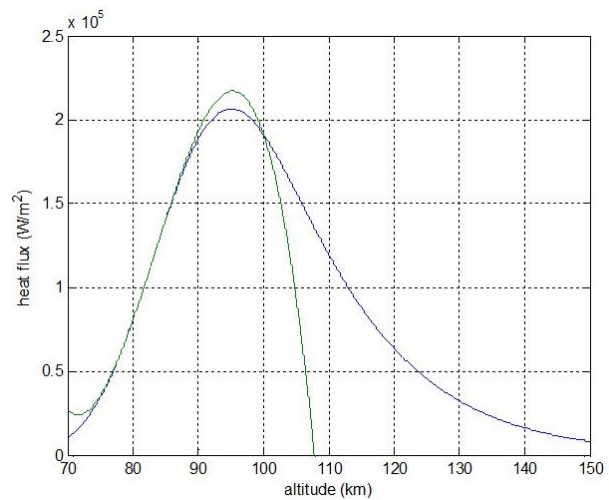
Such a step requires however to assume the sign of the flight path angle; in the present case  $\theta^*$  has been considered as positive downward, and therefore it follows

$$X = \frac{Y \sin \theta_*}{\sqrt{Y^2 - \cos^2 \theta_*}} \quad (35)$$

The analysis to obtain the results presented in the next paragraph has been carried on by expanding  $Y$  and  $U$  up to the 4<sup>th</sup> order in  $\xi$ , and by zeroing the derivative of eq.(26) where these series have been substituted to  $Y$  and  $U$ . At least one of the solutions ends up to be real, and identifies the conditions for the heat peak, representing the condition for the maximum incoming flux. By using the Stefan-Boltzmann relation, i.e.  $q = \sigma \epsilon T^4$  the condition on the heat flux can be transformed to a condition on the maximum temper-



(a) Data points from integration



(b) Approximation by means of a cubic

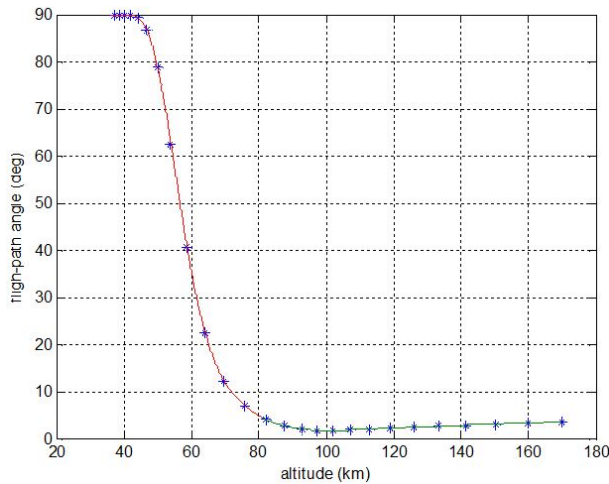
Figure 3. Heat flux along the descent trajectory. Results from complete numerical integration and from proposed approximation are reported.

ature allowed, and either the latter or the previous condition applies to the case of a re-radiating body, i.e. a body that re-emits the incoming heat flux.

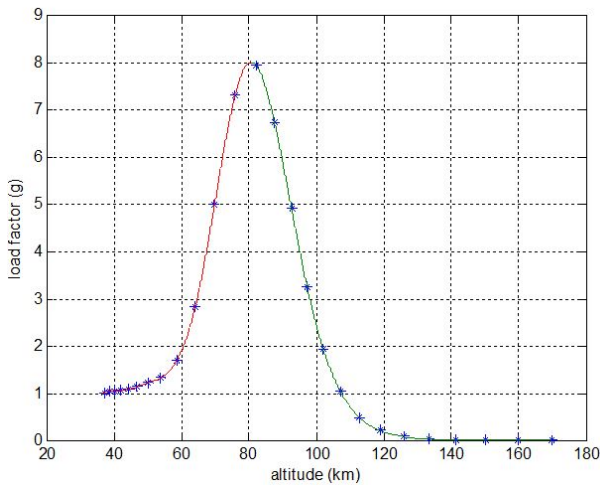
### 3. Results

#### 3.1. No-lift bodies

The first analysis refers to an entrance trajectory with a ratio  $L/D=0$  and a ballistic parameter  $K=0.5$ . Fixing a maximum load factor equal to 8 and a maximum temperature equal to 1400 K (equivalent to  $q=2.1743 \cdot 10^5 \text{ W/m}^2$ ) the relations presented above allow to define a trajectory with an initial flight path angle equal to  $3^\circ$  at the entrance altitude of 170 km, and an entry speed of 8.22 km/s. Following plots (Figure 2) show the behavior of the load factor and of the flight path angle as computed by the proposed technique,



(a) Load factor

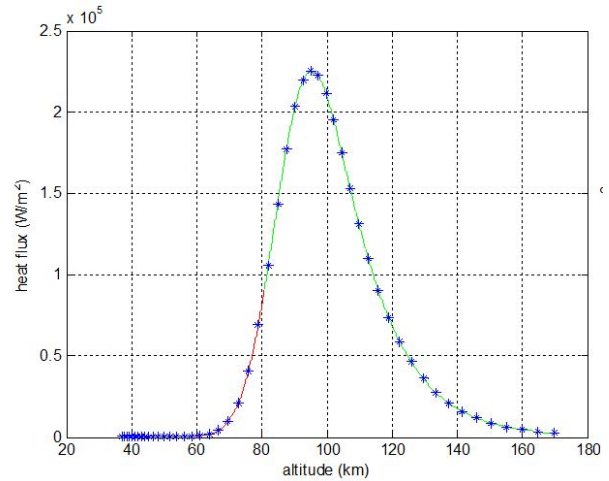


(b) Flight path angle

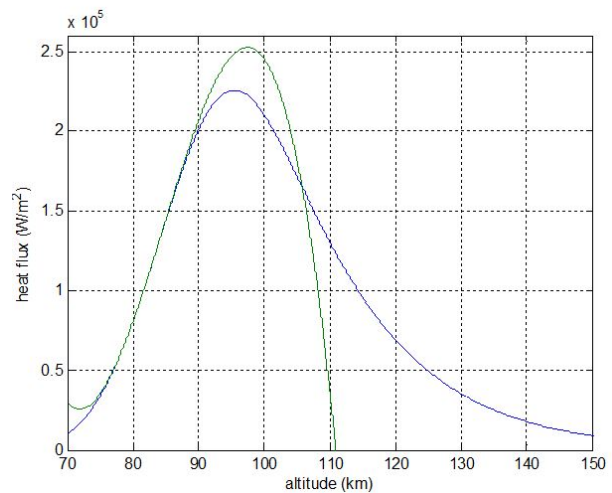
Figure 4. Parameters computed along the trajectory inr a test case where the total heat exchanged has been sepecified (ablative case).

with forward (red curve) and backward (green curve) integration from the load factor peak that is attained at an altitude of 80.363 km (corresponding flight angle  $4.8^\circ$ ). The star marks report the data point of the (forward) integration of the complete set of the equations of motion beginning from the entry point carried on to validate this solution once the initial conditions have been assessed.

Leftmost plot in Figure 3 reports the corresponding behavior of the heat flux, again compared with the data points form a traditional complete integration beginning from the entry conditions. The total heat flux  $Q$  along the descent amounts to  $2.74 \cdot 10^7 \text{ J/m}^2$ . The rightmost plot provides a sketch of the approximation of the flux obtained with the proposed series expansion: it can be noticed how the approximation fits the load peak's neighborhood.



(a) Data points from integration

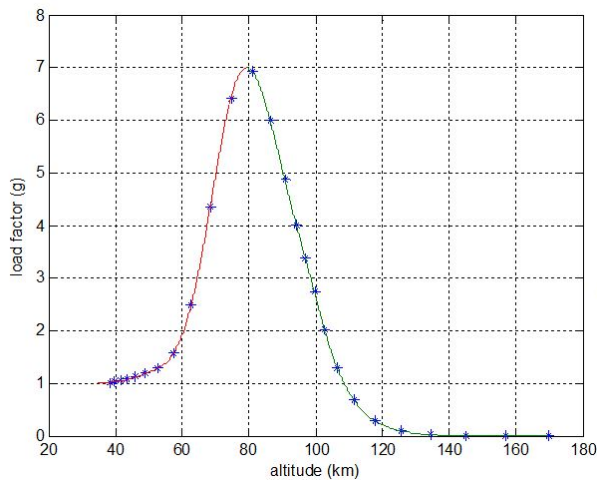


(b) Approximation by means of a cubic

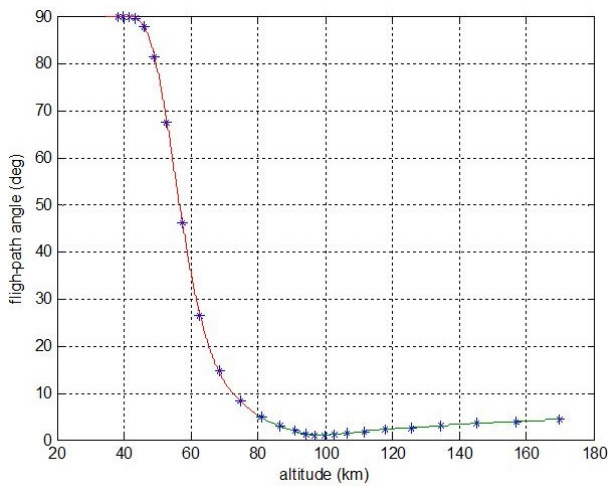
Figure 5. Heat flux along the descent. Results from complete numerical integration and from proposed approximation are reported.

It is also possible, from the previous set of solving relations, to specify the global amount of heat impinging along the descent, instead of the maximum temperature or of the maximum heat flux. This possibility is especially important in case of bodies that manage the heat generated during the re-entry by means of ablation. Following plots (Figures 4 and 5) report the findings for a test case where the peak structural load is still 8, and the total heat has been specified as  $Q = 4 \cdot 10^7 \text{ J/m}^2$ . Corresponding load's peak altitude is 80.806 km (flight angle  $\theta^*=4.55^\circ$ ) and the conditions at the entry (170 km) are flight path angle  $\theta=3.53^\circ$  and speed  $V=8.441 \text{ km/s}$ . Again, the approximation by series expansion matches quite well the behavior close to the peak (Figure 5).

The effect of the variation on the accepted peak load factor is analysed in Figures 6-7, corresponding



(a) Load factor



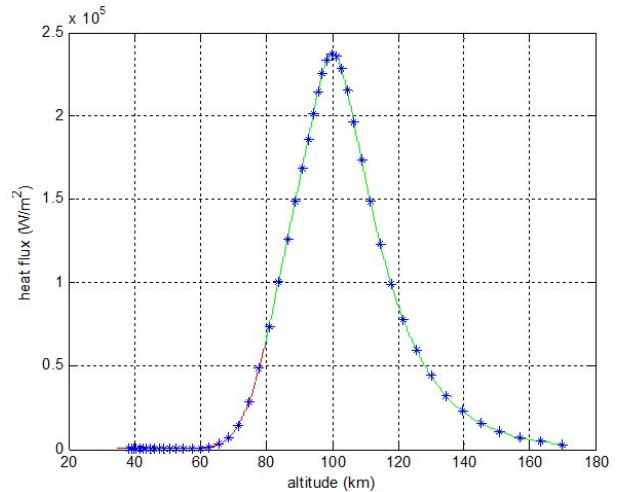
(b) Flight path angle

Figure 6. Parameters computed along the descent trajectory for a test case with peak load assigned and equal to 7.

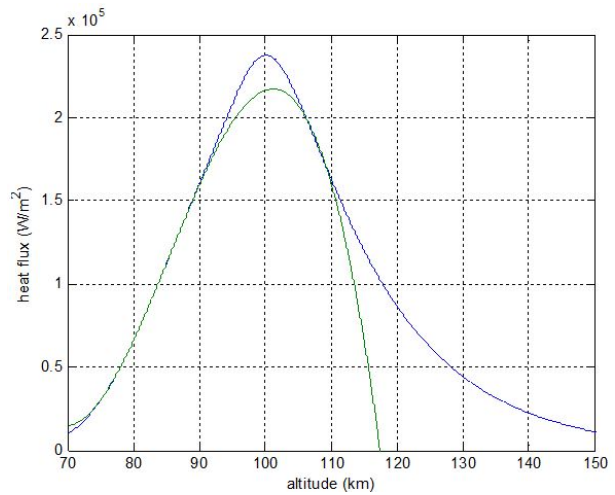
to  $n^*=7$  (as in Figures 2-3, where  $n^*$  was 8, the maximum temperature - 1400 K - is also assigned). As expected, the resulting peak altitude is slightly lower (79.566 km) and the path angle at peak larger ( $5.39^\circ$ ), as well as the total incoming heat  $Q = 3.72 \cdot 10^7 \text{ W/m}^2$ . The conditions at the entry (170 km) are  $4.34^\circ$  (path angle) and 9.113 km/s (speed).

### 3.2. Lifting bodies

The capability to generate lift grants additional degrees of freedom to the designer, and the approach originally proposed by Broglio is capable to manage also this case still beginning from the most important constraints, i.e. the parameters (structural and thermal loads) related to the survivability of the re-entering body, instead that from more vague initial conditions. The test case reported refers to  $L/D$  ratio



(a) Data points from integration



(b) Approximation by means of a cubic

Figure 7. Heat flux along the descent (assigned peak load 7), from numerical integration and from proposed approximation.

equal to 0.1, and still admits a maximum load factor equal to 8 and a maximum temperature equal to 1400 K. Likely, the descent of a lifting body takes a longer time and has a smoother flight path, with the angle at the peak (attained at 85.1 km altitude) equal to  $2.54^\circ$ , beginning with an angle at the entry equal to  $3.21^\circ$ . The computed velocity at the entry point is 7.629 km/s, and the total heat exchanged during the descent amounts to  $1.884 \cdot 10^7 \text{ W/m}^2$ , expectedly lower than in previous cases. The rightmost plot in Figure 9 proves how the proposed expansion fits also in this case the heat flux behavior.

To be noticed how the lifting bodies case requires some special attention as the resulting far less steep trajectory can even end up with an altitude which is not monotonically decreasing in time. In that case (camel-



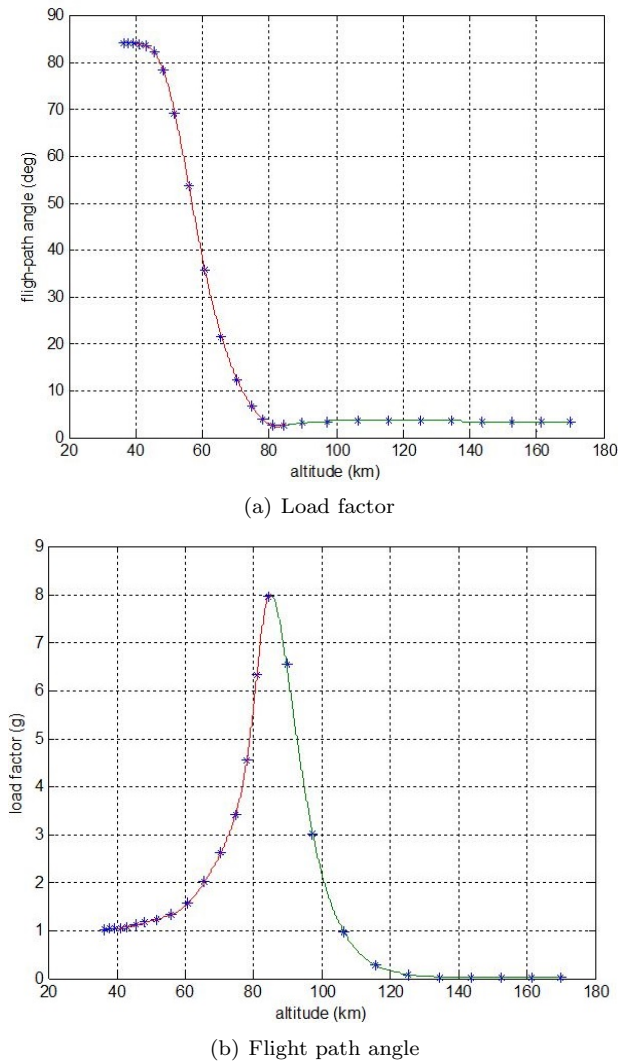


Figure 8. Parameters computed along the trajectory, test case  $L/D=0.1$ .

back trajectory) the backward integration from the peak required by the approach beginning from peak quantities fails, a result which is likely with higher  $L/D$  ratios. Also, this issue explains why the proposed method performs with re-entry from higher terrestrial or interplanetary or lunar transfer orbits better than it does with initial conditions similar to LEOs.

**4. Concluding Remarks**

The paper presents an improvement to the theory proposed by Broglio to compute a re-entry trajectory beginning with the characteristics which are the most important from an engineering point of view, i.e. the maximum structural load and the maximum temperature or heat amount allowed. The improvement is given by an expansion of the non-dimensional functions related to the angular momentum and to the

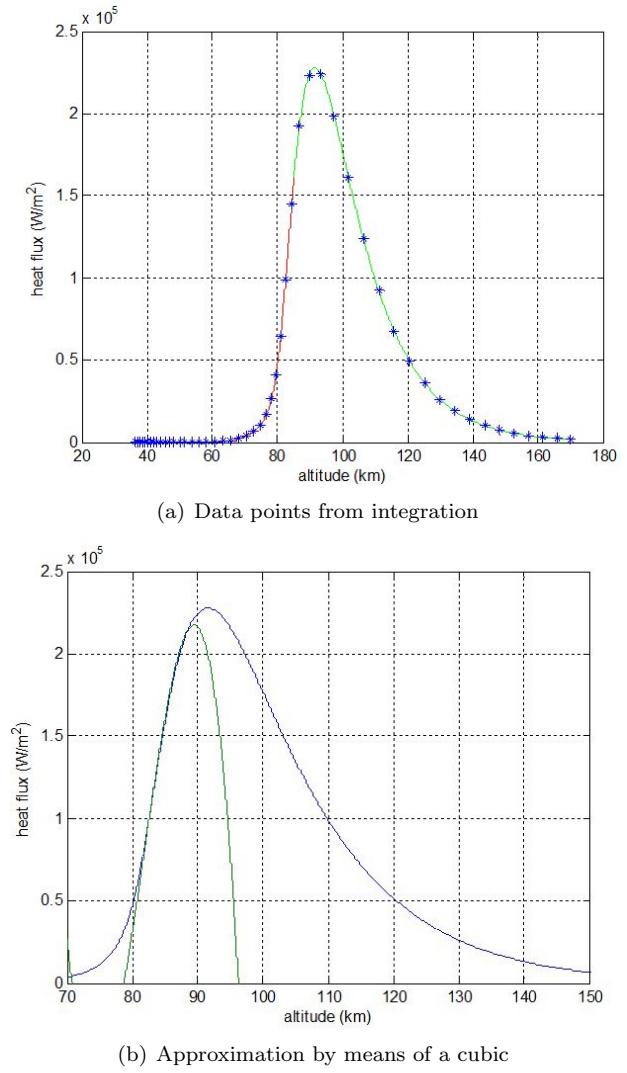


Figure 9. Heat flux from numerical integration and from proposed approximation (case  $L/D=0.1$ ).

flight path angle, which can be represented by a series up to a given order in the neighbourhood of the load's peak altitude. The terms of the expansion can be efficiently computed in a symbolic manner and allow to better define the thermal problem along the descent, increasing and the capabilities of this design technique and its accuracy in representing the most critical phase of the re-entry. These findings are proved by the reported test cases.

**REFERENCES**

1. H. J. Allen, A. J. Jr Eggers, "A Study of the Motion and Aerodynamic Heating of Missiles Entering the Earth's Atmosphere at High Supersonic Speeds", NACA TN-4047, Washington, 1957.
2. D. R. Chapman, "An Approximate Analytical Method for Studying Entry into Planetary Atmospheres", NACA TN-4276, Washington, 1958.

3. S. Sgubini and G. B. Palmerini, "Design of Descent Trajectories in Atmosphere with respect to Engineering Constraints", *IEEE Aerospace Conference Proceedings*, Big Sky (MT), 2004.
4. L. Broglio, "Similar Solutions in Re-Entry Lifting Trajectories", *SIARgraph*, 54, Roma, 1959.
5. L. Broglio, "Re-Entry Trajectories of Space Vehicles", *paper presented in Delft*, 1960.